JACS
JOURNAL OF THE AMERICAN CHEMICAL SOCIETY
Communication
pubs.acs.org/JACS

Substituent Directed Phototransformations of BN-Heterocycles: Elimination vs Isomerization via Selective B−C Bond Cleavage

Deng-Tao Yang,[†] Soren K. Mellerup,[†] Jin-Bao Peng,[†] Xiang Wang,[†] Quan-Song Li,*[,‡] and Suning Wang*[,†,‡]

[†]Department of Chemistry, Queen's University, Kingston, Ontario K7L 3N6, Canada

[‡]Beijing Key Laboratory of Photoelectronic/Electrophotonic Conversion Materials, School of Chemistry, Beijing Institute of Technology, Beijing 100081, P. R. China

Supporting Information

ABSTRACT: Electron-rich and -poor BN-heterocycles with benzyl-pyridyl backbones and two bulky aryls on the boron (Ar = tipp, **BN-1**, Ar = MesF, **BN-2**) have been found to display distinct molecular transformations upon irradiation by UV light. **BN-1** undergoes an efficient photoelimination reaction forming a BN-phenanthrene with Φ_{PE} = 0.25, whereas **BN-2** undergoes a thermally reversible, stereoselective, and quantitative isomerization to a dark colored BN-1,3,5-cyclooctatriene (BN-1,3,5-COT, **BN-2a**). This unusual photoisomerization persists for other BN-heterocycles with electron-deficient aryls such as **BN-3** with a benzyl-benzothiazolyl backbone and Mes^F substituents or **BN-4** with a benzyl-pyridyl backbone and two C_6F_5 groups on the boron. The photoisomerization of **BN-4** goes beyond BN-1,3,5-COT (**BN-4a**), forming a new species (BN-1,3,6-COT, **BN-4b**) via C−F bond cleavage and [1,3]-F atom sigmatropic migration. Computational studies support that **BN-4a** is an intermediate in the formation of **BN-4b**. This work establishes that steric and electronic factors can effectively control the transformations of BN-heterocycles, allowing access to important and previously unknown BN-embedded species.

Controlling the fate of chemical transformations is one of the cornerstones of modern chemistry and biology. Although nature has achieved this feat by employing molecular architectures (e.g., enzymes),[1] chemists rely heavily on manipulating the steric and electronic factors of small molecules/complexes[2] to promote desired reaction outcomes. For example, steric/electronic considerations have proven highly effective in both the stabilization of rare chemical entities[3] as well as the facilitation of unique molecular transformations.[4] Recently, similar strategies have been applied to organoboron systems, which has demonstrated the remarkable breadth of varying reactivity and functions available to these species[5] (e.g., optoelectronics,[5b,h] catalytic components,[5i,l] organic synthons,[5m,q] etc). We have had a long-standing interest in the photoresponsive properties of organoboron compounds[6,7] and have previously shown that BN-heterocycles such as **BN-0** (R = Me, X = H; Scheme 1) are capable of undergoing photoelimination of mesitylene to produce fully conjugated and highly luminescent BN-phenanthrenes (**BN-phen**).[6d] Although this transformation does provide a new method of preparing these BN-phenanthrene isomers and allow for the in situ generation of optoelectronic devices such as OLEDs based on such BN-systems,[7] the low quantum efficiency of the photoreaction ($\Phi_{PE} \leq$ 0.044) severely limits its synthetic and practical usefulness. Inspection of the DFT-calculated transition state for this reaction revealed that B−C_{Ar} bond breaking is likely the rate-limiting step.[6f] Therefore, we postulated that weakening the B−C_{Ar} bond through either greater steric encumberment, i.e., replacing the Mes groups in **BN-0** with 2,4,6-triisopropylphenyl (tipp, **BN-1**) or bulky/strongly electron-withdrawing groups such as 2,4,6-trifluoromethylphenyl (Mes^F, **BN-2**), could improve the efficiency of the photoelimination. Indeed, this strategy proved successful with respect to **BN-1**, which eliminated much more efficiently than **BN-0**. However, instead of elimination, **BN-2** exhibited an unprecedented photochromic switching around the boron core, generating an intensely colored and previously unknown BN-1,3,5-cyclooctatriene (COT). Further investigation revealed that the photochemical formation of BN-1,3,5-COT is a general phenomenon for BN-heterocycles with electron-deficient aryl groups on boron, establishing the possibility to control such molecular transformations by tuning the steric and electronic properties of the molecule. The details of the two distinct phototransformations and mechanistic insights are presented herein.

Scheme 1. Substituent-Directed Transformations of BN-Heterocycles

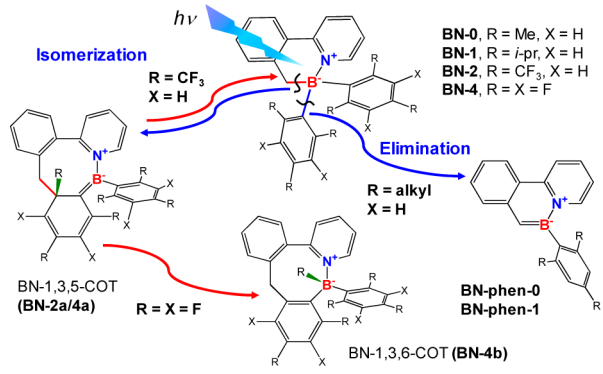

Received: August 6, 2016
Published: August 31, 2016

DOI: 10.1021/jacs.6b07899
J. Am. Chem. Soc. 2016, 138, 11513−11516

Compounds **BN-1** and **BN-2** were prepared using a modified procedure[6d] for **BN-0** and the corresponding in situ generated Ar_2BX (X = F, Cl) reagents. Both were fully characterized by ^{1}H, ^{13}C, ^{11}B, and ^{19}F NMR, HRMS, and single crystal X-ray diffraction analyses (see SI). Crystal data revealed that the B−C_{Ar} bonds of **BN-1** and **BN-2** are about 0.02 Å longer than those of **BN-0**, whereas all three B−CH_2 bond lengths are comparable. The DFT-calculated B−C_{Ar} lengths match well with those determined experimentally, with the calculated B-Mes^F lengths in **BN-2** being ∼0.01 Å longer than those of B-tipp in **BN-1**. This difference highlights the strong withdrawing nature of Mes^F in addition to its steric bulk.

The photoreactivity of **BN-1** in solution and polymer films is similar to that of **BN-0**, with the brightly green fluorescent **BN-phen-1** (λ_{em} = 500 nm, Φ_{FL} = 0.27) formed quantitatively upon irradiation at 300 nm as evidenced by UV−vis, NMR, and crystal structure data (see SI). The most striking difference between **BN-0** and **BN-1** is the Φ_{PE} which was determined to be 0.25 for **BN-1** using competitive NMR photolysis experiments (SI) ca. 6 times greater than that of **BN-0** (0.044), exceptionally high for a photoelimination reaction. The weaker B-tipp bonds of **BN-1** are clearly responsible for this significant enhancement in photoelimination efficiency. This demonstrates that the use of bulkier electron rich aryl groups on boron is an effective strategy for achieving highly efficient aryl-elimination in such systems, thus making the use of BN-heterocycles as precursors for in situ fabrication of azaborine-based optoelectronic devices[7] more viable.

Despite a similarly congested structure and long B-Mes^F bonds, **BN-2** does not undergo photoelimination. Irradiation (300 nm) of **BN-2** in C_6D_6 or THF resulted in the rapid and clean conversion of **BN-2** to a new species, **BN-2a**, which has sharp and well-resolved peaks in the ^{1}H NMR spectrum and a ^{11}B chemical shift at ∼35 ppm, typical of a three-coordinated boron with one unsaturated bond[8] (Figure 1b and SI). Accompanying the NMR spectral change was a dramatic change in solution color from colorless to dark orange-brown (Figure 1). In the UV−vis spectrum, a broad low energy absorption band at λ_{max} = 433 nm (Figure 1d) appears with irradiation. TD-DFT data suggests that the low energy band of **BN-2a** originates from a charge transfer (CT) transition from HOMO located on the π-system of the B═C and the cyclohexandiene moiety to LUMO (π^*) located on the py ring of the backbone (SI). Remarkably, heating the orange-brown solution at 90 °C resulted in full recovery of **BN-2** by NMR and restoration of the original solution color. The activation energy of this process was ∼33.3 kcal/mol (SI). **BN-2a** forms dark orange-brown crystals, allowing us to establish its structure by X-ray diffraction.

The crystal structure of **BN-2a** (Figure 2) revealed a previously unknown BN-embedded cyclic structure, which is formally a 4,5-dihydro-1,2-azaborocine but will be described as BN-1,3,5-cyclooctatriene (BN-1,3,5-COT) for convenience. The CH_2 group in **BN-2a** is no longer bound to the boron atom, but instead forms a C−C bond with one CF_3-substituted quaternary carbon atom (C(14)) of a Mes^F ring. This converts the Mes^F to a 1,3-cyclohexadiene and the B—C bond to a B═C bond (1.465(3) Å), with similar length compared to previously reported B═C bonds.[8] Comparing the structure of **BN-2a** to the photoproduct of previously reported B(ppy)Mes_2,[6a−d] which forms a tricyclic 1,2-azaboratabisnorcaradiene, it is clear that the switching described for **BN-2** represents a new class of photochromic materials. The Φ_{PE} of **BN-2** to **BN-2a** transformation was determined to be 0.23 (SI). BN-1,3,5-COTs are a

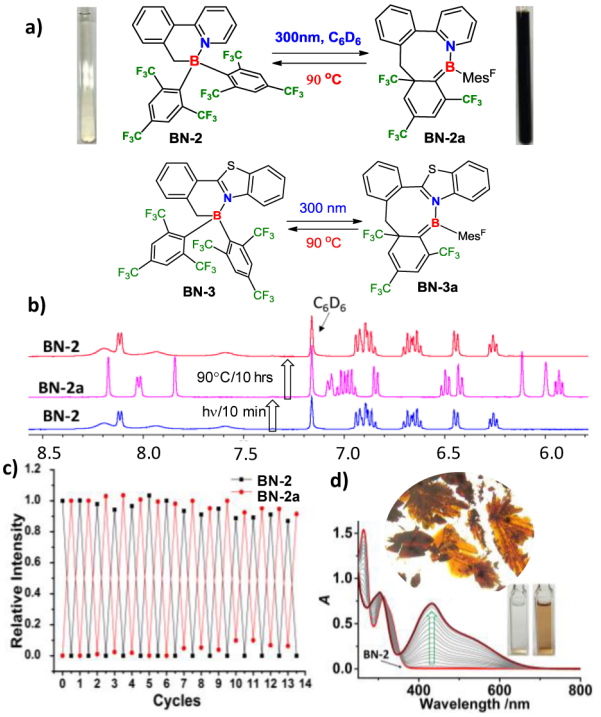

Figure 1. (a) Scheme showing the interconversion of **BN-2**/**BN-3** and **BN-2a**/**BN-3a**. (b) ^{1}H NMR spectra showing the photo (300 nm) and thermal (90 °C) interconversion of **BN-2** and **BN-2a** in C_6D_6. (c) Diagram showing the fatigue resistance of the **BN-2** and **BN-2a** with the irradiation and heating cycles using integrated peak intensity relative to the C_6D_6 peak in ^{1}H NMR spectra (Figure S3.3). (d) UV−vis spectra showing the conversion of **BN-2** to **BN-2a** in THF (1×10^{-4} M) and photographs showing the crystals of **BN-2a** and solution color of **BN-2** and **BN-2a**.

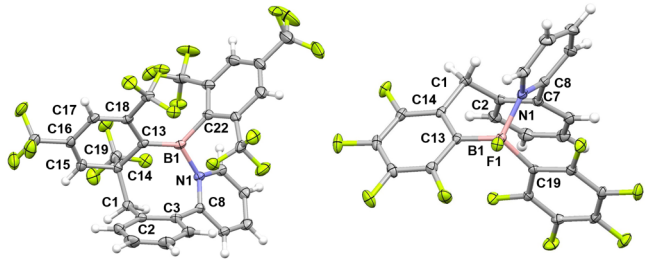

Figure 2. Crystal structures of **BN-2a** (left), **BN-4b** (right).

previously unknown class of BN-embedded molecules. The clean and quantitative generation of **BN-2a** via the photoisomerization of **BN-2** provides a convenient method for accessing such unusual species. Furthermore, despite **BN-2a** having a chiral carbon atom (C(14)) and chiral COT structure, only one diastereoisomer was observed by NMR in which the CF_3 (C(19)) is *syn* to the py ring whereas the phenyl and the cyclohexadienyl of the COT unit are *syn* to each other. Thus, the **BN-2** to **BN-2a** transformation proceeds with high stereoselectivity.

To demonstrate the robustness of this discovered photochromic system, the fatigue resistance of **BN-2** was examined by cycling through the **BN-2**→**BN-2a**→**BN-2** transformations repeatedly. Remarkably, the continuous photothermal cycling between these two states did not yield any appreciable decomposition until the 13th cycle as shown by ^{1}H NMR data (Figure 1c and SI), indicating that **BN-2**/**BN-2a** possess excellent

DOI: 10.1021/jacs.6b07899
J. Am. Chem. Soc. 2016, 138, 11513−11516

fatigue resistance. This feature makes these systems promising for future applications involving molecular switches.

To establish if the new phototransformation is available to other BN-heterocycles with different chelate backbones, **BN-3**, an analogue of **BN-2** with a 2-benzyl-benzothiazolyl backbone, was prepared (Figure 1). Upon irradiation at 300 nm, **BN-3** undergoes a similar photoswitching as observed for **BN-2** (see SI), forming a deep brown colored **BN-3a**, an analogue of **BN-2a**, according to its diagnostic ^{1}H, ^{11}B, and ^{19}F NMR spectra. Again, only one diastereoisomer was observed. **BN-3a** possesses a low energy absorption band with λ_{max} = 458 nm in its UV−vis spectrum, which is red-shifted by ∼25 nm compared to **BN-2a**, consistent with the greater π-conjugation of the backbone in **BN-3a**. The Φ_{PE} of **BN-3** to **BN-3a** transformation was determined to be 0.10. Thermally, **BN-3a** converts back to the colorless **BN-3** at 90 °C with ∼5% decomposition observed in the process (see SI). This example shows that the new photochromic phenomenon is not limited to systems with a benzyl-pyridyl backbone.

Given the bulky nature of the aryl groups in **BN-1**, **BN-2**, and **BN-3**, but their distinctly different photoreactivity, the electron-deficiency of Mes^{F} appears to be pivotal for the new photochromism. To probe this hypothesis, the photoreactivity of **BN-4**,[6f] which has the same backbone as **BN-2** and two less sterically congested but comparably electron-withdrawing C_6F_5 substituents, was examined. Upon irradiation of **BN-4** at 300 nm, no obvious color change was observed. However, ^{1}H, ^{19}F, and ^{11}B NMR revealed the quantitative formation of a new species, **BN-4b**, with a typical four-coordinated ^{11}B chemical shift of 5.6 ppm (Figure 3 and SI). Single-crystal X-ray diffraction analysis

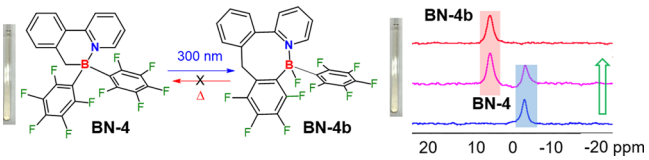

Figure 3. Irreversible photoisomerization of **BN-4** and the ^{11}B NMR spectra in C_6D_6 showing full conversion of **BN-4** (blue) to **BN-4b** (red).

established that **BN-4b** shares some structural similarities with **BN-2a**/**3a** and may be described as a BN-embedded 1,3,6-COT, an isomer of BN-1,3,5-COT (Figure 2). The key difference between **BN-2a**/**3a** and **BN-4b** is that the third double bond in the latter is not conjugated with the other two in the COT ring, and the boron center is four-coordinated with a B−F bond. As a consequence, **BN-4b** has no low energy absorption band in the visible region, which is consistent with TD-DFT calculated data (SI). The B atom in **BN-4b** is a chiral center, which, combined with the chiral COT structure, creates the possibility of diastereomers. The fact that only one diastereomer was observed in which the B−F bond is *syn* to the py ring (Figure 2) supports that the **BN-4** to **BN-4b** transformation also has high stereoselectivity. Unlike **BN-2a**/**3a**,which can thermally revert to **BN-2**/**3**, **BN-4b** is thermally stable and does not convert back to **BN-4**. Given the bond energy of the C−F bond,[9] its cleavage in the **BN-4** to **BN-4b** transformation is highly unusual and interesting, which may be driven by the stability of **BN-4b**.

To understand the unusual photoisomerization of **BN-2**/**4**, DFT and TD-DFT calculations were performed for each with the complete reaction pathway of **BN-4** shown in Figure 4. Excitation at 300 nm populates the S_1 state of **BN-4** at the Franck−Condon (FC) structure, which is of $\pi\pi^*$ character and mainly arises from its HOMO to LUMO transition. Relaxation leads to a minimum

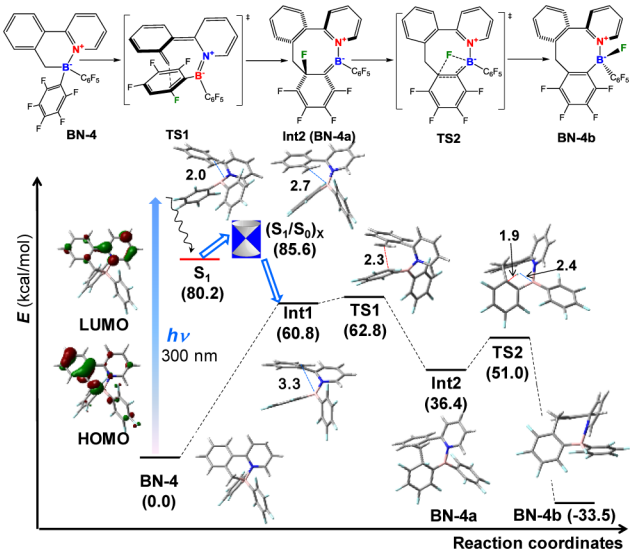

Figure 4. Calculated potential energy profile for the photoisomerization of **BN-4**. The energies of the all key species, as well as the intersection point of the S_0 and S_1 state ($(S_1/S_0)_X$) are relative to **BN-4** and given in the parentheses. Some key distances (in Å) and the HOMO/LUMO orbitals of **BN-4** are also shown.

in the S_1 state, which is close in energy (∼5 kcal mol^{-1}) to a conical intersection point $(S_1/S_0)_X$ between the S_1 and S_0 states, therefore allowing access to the ground state from the excited state.[10] In the S_0, S_1, and $(S_1/S_0)_X$ structures, the B−CH_2 distances are 1.6, 2.0, and 2.7 Å, respectively, indicating that the B−CH_2 is broken upon photoexcitation. At $(S_1/S_0)_X$, the excited state decays to the ground state and the reaction path leads to an intermediate (Int1) with a B−CH_2 distance of 3.3 Å, a negatively charged (−0.44 e) CH_2 carbon atom, and a positively charged (+0.29 e) *o*-carbon of one C_6F_5 ring. The latter two moieties have a separation distance of 2.3 Å at the TS1 state, with perfect orientation for C−C bond formation or electrocyclization similar to that observed in a reported photochromic boron system,[11] generating Int2 (**BN-4a**), an analogue of **BN-2a**. The TS1 state lies only 2 kcal/mol above Int1, suggesting that the reaction from Int1 to **BN-4a** occurs readily. Unlike **BN-2a**, which does not undergo further isomerization, the F atom of **BN-4a** can migrate from carbon to boron by overcoming a barrier of ∼15 kcal/mol at the TS2 state forming **BN-4b**, which resembles the classic transition state structure proposed for 1,3-sigmatropic shifts, leading to the selective formation of one diastereoisomer.[9c] The attraction between the F atom and the electron deficient B atom clearly favors the rearrangement from **BN-4a** to **BN-4b**, which is −33.5 kcal/mol lower in energy than **BN-4**. These data support that the formation of **BN-4b** is thermodynamically favorable and the reverse reaction is prohibited due to the large reverse barrier of 96.3 kcal/mol. Due to the large size of **BN-2** and its analogous isomerization pathway, only the ground-state reaction pathway was determined. The key transition state of **BN-2** has a similar TS1 structure as **BN-4**, with C−C distance between CH_2 and C_{CF3} of 2.4 Å (SI). The calculated barrier for **BN-2a** reverting back to **BN-2** is 34.2 kcal/mol, which agrees with the experimental value of 33.3 kcal/mol. The fact that the BN-1,3,6-COT isomer was not observed for **BN-2** may be explained by an unfavorable transition state caused by steric crowding of the bulky CF_3 groups. The calculated reaction pathway also corroborates the stereoselective formation of **BN-2a** and **BN-4b**.

DOI: 10.1021/jacs.6b07899
J. Am. Chem. Soc. 2016, 138, 11513−11516

One key feature revealed by DFT data is that the HOMO of **BN-2** and **BN-4** is localized mainly on the benzyl ring of the chelate backbone and the B atom with very little contributions from the Mes^F or C_6F_5 groups. This is in contrast to **BN-0** and **BN-1**, in which the HOMO is made of almost exclusively π orbitals on the Mes and tipp groups (Figure S6.1e). The substituent groups on the aryl rings are clearly responsible for this difference between the electron-rich and electron-poor BN-heterocycles, which led to their distinct photoreactivity (i.e., aryl-elimination vs $-CH_2$ migration/isomerization). The electron-withdrawing Mes^F and C_6F_5 likely contribute to the stabilization of the TS1 state by strengthening the B═N bond. This stabilization effect by Mes^F substitution is reminiscent of that reported for borole systems[12a] and conjugated thienylborane systems.[12b] Further evidence to support the importance of electron-deficient aryl groups in the photoisomerization of BN-heterocycles are provided by the photostability of **BN-5** (replacing one C_6F_5 in **BN-4** by a phenyl ring) and **BN-6** (replacing both C_6F_5 in **BN-4** by two phenyl rings), which do not show any change under 300 nm irradiation for up to 48 h (SI).

In summary, both electronic and steric effects have a significant and distinct impact on the photoreaction pathways of BN-heterocycles. With bulky, electron-donating aryl rings on the B atom, the photoelimination efficiency is enhanced. In contrast, with sufficiently electron-withdrawing aryl groups on the B atom, bulky or not, photoisomerization occurs exclusively with high stereoselectivity. Bulky electron-withdrawing aryl groups such as Mes^F appear to be the key for reversible photothermal isomerization of this class of photochromic molecules. Balancing steric and electronic factors is critical for achieving the desired molecular transformations based on BN-heterocycles. The first examples of BN-1,3,5-COT and BN-1,3,6-COT molecules have been obtained, and their relationship in structural transformation has been demonstrated.

■ ASSOCIATED CONTENT

Supporting Information

The Supporting Information is available free of charge on the ACS Publications website at DOI: 10.1021/jacs.6b07899.

Spectroscopic data for new compounds, experimental and computational details, crystal structural data, (PDF)
Data for $C_{42}H_{56}BN$ (CIF)
Data for $C_{27}H_{32}BN$ (CIF)
Data for $C_{30}H_{14}BF_{18}N$ (CIF)
Data for $C_{60}H_{28}B_2F_{36}N_2$ (CIF)
Data for $C_{24}H_{10}BF_{10}N$ (CIF)
Data for $C_{24}H_{15}BF_5N$ (CIF)
Data for $C_{24}H_{20}BN$ (CIF)

■ AUTHOR INFORMATION

Corresponding Authors

*S.W. wangs@chem.queensu.ca
*Q.-S.L. liquansong@bit.edu.cn

Notes

The authors declare no competing financial interest.

■ ACKNOWLEDGMENTS

The authors thank the Natural Science and Engineering Research Council of Canada (RGPIN1193993-2013) and the National Natural Science Foundation of China for Financial support (grants 21571017 and 21303007). S.K.M. thanks the Canadian Government for the Vanier Scholarship.

■ REFERENCES

(1) (a) *Microbial Enzymes and Biotechnology*, 2nd ed; Fogarty, W. M., Kelly, C. T., Eds.; Springer Applied Science: New York, 2012. (b) *Molybdenum and Molybdenum-Containing Enzymes*; Coughlan, M. P., Ed.; Pergamon Press, Willowdale, 1980. (c) *Immobilized Enzymes for Industrial Reactors*; Messing, R. A., Ed.; Academic Press: New York, 1975.

(2) (a) Grubbs, R. H.; Chang, S. *Tetrahedron* **1998**, *54*, 4413. (b) Schrock, R. R. *Tetrahedron* **1999**, *55*, 8141. (c) Anderson, J. S.; Rittle, J.; Peters, J. C. *Nature* **2013**, *501*, 84.

(3) (a) Braunschweig, H.; Dewhurst, R. D.; Schneider, A. *Chem. Rev.* **2010**, *110*, 3924. (b) Soleilhavoup, M.; Bertrand, G. *Acc. Chem. Res.* **2015**, *48*, 256. (c) Martin, C. D.; Soleilhavoup, M.; Bertrand, G. *Chem. Sci.* **2013**, *4*, 3020.

(4) (a) Berkovic, G.; Krongauz, V.; Weiss, V. *Chem. Rev.* **2000**, *100*, 1741. and references therein. (b) Irie, M. *Chem. Rev.* **2000**, *100*, 1685. (c) Ko, C.-C.; Yam, V. W.-W. *J. Mater. Chem.* **2010**, *20*, 2063.

(5) (a) *Boron Science New Technologies and Applications*; Hosmane, N. S., Ed.; CRC, Taylor & Francis: Boca Raton, 2012. (b) Entwistle, C. D.; Marder, T. B. *Chem. Mater.* **2004**, *16*, 4574. (c) Wakamiya, A.; Taniguchi, T.; Yamaguchi, S. *Angew. Chem., Int. Ed.* **2006**, *45*, 3170. (d) Chen, P.; Lalancette, R. A.; Jäkle, F. *Angew. Chem., Int. Ed.* **2012**, *51*, 7994. (e) Lorbach, A.; Hübner, A.; Wagner, M. *Dalton Trans.* **2012**, *41*, 6048. (f) Escande, A.; Ingleson, M. J. *Chem. Commun.* **2015**, *51*, 6257. (g) Wang, X.-Y.; Wang, J.-Y.; Pei, J. *Chem. - Eur. J.* **2015**, *21*, 3528. (h) Li, D.; Zhang, H.; Wang, Y. *Chem. Soc. Rev.* **2013**, *42*, 8416. (i) Stephan, D. W.; Erker, G. *Angew. Chem., Int. Ed.* **2015**, *54*, 6400. (j) McGough, J. S.; Butler, S. M.; Cade, I. A.; Ingleson, M. J. *Chem. Sci.* **2016**, *7*, 3384. (k) Süsse, L.; Hermeke, J.; Oestreich, M. *J. Am. Chem. Soc.* **2016**, *138*, 6940. (l) *Boronic acids*; Hall, D. G., Ed.; Wiley-VCH: Weinheim, 2005. (m) Brown, H. C. *Boranes in Organic Chemistry*; Cornell University Press: Ithaca, 1972. (n) Suzuki, A. *Heterocycles* **2010**, *80*, 15. (o) Campbell, P. G.; Marwitz, A. J. V.; Liu, S.-Y. *Angew. Chem., Int. Ed.* **2012**, *51*, 6074. (p) Bosdet, M. J. D.; Piers, W. E. *Can. J. Chem.* **2009**, *87*, 8. (q) Molander, G. A. *J. Org. Chem.* **2015**, *80*, 7837.

(6) (a) Rao, Y.-L.; Amarne, H.; Zhao, S.-B.; McCormick, T. M.; Martić, S.; Sun, Y.; Wang, R.-Y.; Wang, S. *J. Am. Chem. Soc.* **2008**, *130*, 12898. (b) Rao, Y.-L.; Amarne, H.; Wang, S. *Coord. Chem. Rev.* **2012**, *256*, 759. (c) Rao, Y.-L.; Hörl, C.; Braunschweig, H.; Wang, S. *Angew. Chem., Int. Ed.* **2014**, *53*, 9086. (d) Lu, J.-S.; Ko, S.-B.; Walters, N. R.; Kang, Y.; Sauriol, F.; Wang, S. *Angew. Chem., Int. Ed.* **2013**, *52*, 4544. (e) Ko, S.-B.; Lu, J.-S.; Wang, S. *Org. Lett.* **2014**, *16*, 616. (f) Yang, D.-T.; Mellerup, S. K.; Wang, X.; Lu, J.-S.; Wang, S. *Angew. Chem., Int. Ed.* **2015**, *54*, 5498.

(7) Wang, S.; Yang, D.-T.; Lu, J.; Shimogawa, H.; Gong, S.; Wang, X.; Mellerup, S. K.; Wakamiya, A.; Chang, Y.-L.; Yang, C.; Lu, Z. H. *Angew. Chem., Int. Ed.* **2015**, *54*, 15074.

(8) (a) Paetzold, P.; Englert, U.; Finger, R.; Schmitz, T.; Tapper, A.; Ziembinski, R. *Z. Anorg. Allg. Chem.* **2004**, *630*, 508. (b) Hunold, R.; Pilz, M.; Allwohn, J.; Stadler, M.; Massa, W.; Schleyer, P. V. R.; Berndt, A. *Angew. Chem., Int. Ed. Engl.* **1989**, *28*, 781. (c) Pilz, M.; Stadler, M.; Hunold, R.; Allwohn, J.; Massa, W.; Berndt, A. *Angew. Chem., Int. Ed. Engl.* **1989**, *28*, 784. (d) Pilz, M.; Michel, H.; Berndt, A. *Angew. Chem., Int. Ed. Engl.* **1990**, *29*, 401.

(9) (a) Klahn, M.; Rosenthal, U. *Organometallics* **2012**, *31*, 1235. (b) Caputo, C. B.; Hounjet, L. J.; Dobrovetsky, R.; Stephan, D. W. *Science* **2013**, *341*, 1374. (c) Nair, N. G.; Mendoza-Cortes, J. L.; Abrol, R.; Goddard, W. A., III; Reddy, V. P. *J. Organomet. Chem.* **2013**, *747*, 133.

(10) (a) Polli, D.; Altoe, P.; Weingart, O.; Spillane, K. M.; Manzoni, C.; Brida, D.; Tomasello, G.; Orlandi, G.; Kukura, P.; Mathies, R. A.; Garavelli, M.; Cerullo, G. *Nature* **2010**, *467*, 440. (b) Blancafort, L. *ChemPhysChem* **2014**, *15*, 3166.

(11) Iida, A.; Saito, S.; Sasamori, T.; Yamaguchi, S. *Angew. Chem., Int. Ed.* **2013**, *52*, 3760.

(12) (a) Zhang, Z.; Edkins, R. M.; Haehnel, M.; Wehner, M.; Eichhorn, A.; Mailänder, L.; Meier, M.; Brand, J.; Brede, F.; Müller-Buschbaum, K.; Braunschweig, H.; Marder, T. B. *Chem. Sci.* **2015**, *6*, 5922. (b) Yin, X.; Chen, J.; Lalancette, R. A.; Marder, T. B.; Jäkle, F. *Angew. Chem., Int. Ed.* **2014**, *53*, 9761.

DOI: 10.1021/jacs.6b07899
J. Am. Chem. Soc. 2016, 138, 11513−11516